ACS Energy LETTERS

http://pubs.acs.org/journal/aelccp

LETTER

Minimal Effect of the Hole-Transport Material Ionization Potential on the Open-Circuit Voltage of Perovskite Solar Cells

Rebecca A. Belisle, Pratham Jain, Rohit Prasanna, Tomas Leijtens, and Michael D. McGehee*

Materials Science & Engineering Department, Stanford University, Stanford, California 94305, United States

Supporting Information

ABSTRACT: **Hole-transport material optimization is an important step toward maximizing the efficiency of perovskite solar cells. Here, we investigate the role of one hole-transport material property, the ionization potential, on the performance of perovskite solar cells. We employ a device architecture that allows us to systematically tune the ionization potential while avoiding any impact to other device parameters, and we find that for a wide range of ionization potentials the photovoltaic performance is minimally affected. This finding relaxes the requirement for the development of hole-transport materials with particular ionization potentials, allowing for the optimization of hole-transport materials that can improve performance in differing ways such as through increased stability or decreased parasitic absorption.**

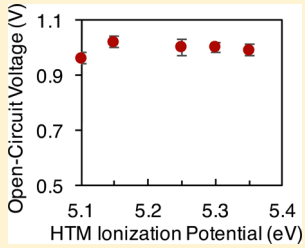

In a brief moment in the history of solar cells, perovskite solar cells have risen from a humble improvement of dye-sensitized solar cells to highly studied and specialized devices that have more in common with thin-film solar cell technologies than with their dye predecessors. Through advances in materials processing, chemistry, and device engineering, power conversion efficiencies for devices made with hybrid perovskites have quickly climbed above 20%.[1−7] However, despite all of these advances, some components of the perovskite solar cell have remained relatively unimproved. Notably, six years after their original implementation, most perovskite solar cells still use spiro-OMeTAD as the default hole-transport material (HTM),[8,9] which is surprising given the tremendous interest in developing novel HTMs for improved perovskite solar cell efficiency and stability.[10,11] This encourages an investigation into the specific design parameters that make some HTMs better than others for high-efficiency perovskite solar cells, with the objective of identifying a better-performing HTM than spiro-OMeTAD.

One significant HTM design parameter is the ionization potential (IP). There are many groups that attribute improvements in the photovoltage of perovskite solar cells to increasing the IP of the HTM.[12−20] Several researchers, including Polander et al. and Kulbak et al., have varied HTMs and see improvements in V_{OC} for iodide- and bromide-containing perovskites, respectively, that correlate with increasing IP.[12,19] These studies have strongly encouraged the design and implementation of new HTMs with IPs that more closely match the $MAPbI_3$ valence band near −5.4 eV.[21,22] However, as of yet, none of these new HTMs have been incorporated into devices with higher V_{OC} than champion devices made with spiro-OMeTAD[7] (which has a lower IP, between 5.0 and 5.2 eV depending upon doping[21,23]). Additionally, a recent report from Abate et al. showed similar efficiency for two devices made with HTMs of significantly different IPs.[24] These results call into question whether tuning the IP is indeed necessary for improved performance. To better understand the role of the HTM and how to optimize it, our work undertakes a systematic investigation of the effects of varying HTM IP on perovskite solar cell performance.

A complication in determining the role of the HTM IP on device performance is that changing the HTM often affects multiple facets of the solar cell, all of which can have a significant impact on photovoltaic performance. When the perovskite is deposited on top of the HTM in an "inverted" architecture, the HTM serves as a substrate and significantly affects the perovskite morphology and grain size in addition to acting as a selective contact.[12,25,26] For HTMs deposited on top of the perovskite, solution processing can result in additional complications such as variations in the HTM film uniformity that may affect the shunting of the devices.[18,19,24] Solvent-annealing or surface passivation of the perovskite from HTM additives can obscure the effects of changing the IP of the HTM.[27] Additionally, HTMs may have varying selectivity (as determined by the semiconductor band gap), which should affect performance.[28] In this study, we construct a device architecture that allows us to tune the IP of the HTM while minimally impacting any other device parameter to elucidate the true impact of the IP on the performance of $CH_3NH_3PbI_3$ perovskite solar cells. We evaporate a series of HTMs on top of

Received: July 12, 2016
Accepted: August 15, 2016
Published: August 15, 2016

DOI: 10.1021/acsenergylett.6b00270
ACS Energy Lett. 2016, 1, 556−560

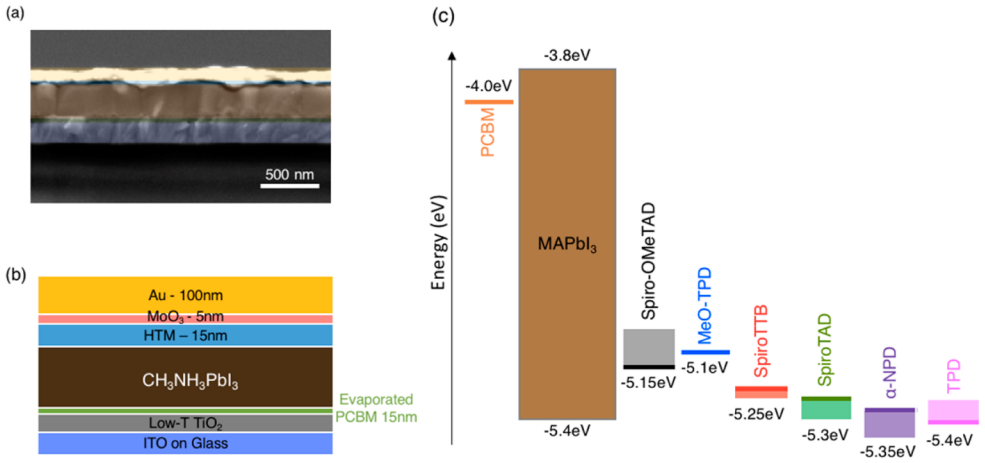

Figure 1. Cross-sectional SEM of the perovskite solar cell used in this study (a) and the associated device schematic (b). Architecture was employed for all evaporated HTMs with varying IPs as determined by photoemission spectroscopy in air (PESA) (c). Solid lines under HTMs show HOMO values measured by PESA, while boxes represent the range of HOMO values previously reported for these materials.[12,21,31]

the perovskite, and in doing so, we find similar photovoltages for devices made with HTMs of widely varying IPs. These results suggest that the IP should not be the principal design constraint when developing novel HTMs, but instead, properties such as minimized parasitic absorption, beneficial-processing, and effects on perovskite morphology should be optimized to maximize perovskite device efficiency.

The device architecture for this study, depicted in Figure 1, was optimized for reproducibility as well as minimization of undesirable effects of the HTM deposition. A 15 nm layer of phenyl-C_{61}-butyric acid methyl ester (PCBM) was deposited on top of TiO_2 to act as a reproducible and low-hysteresis electron-transport layer (ETL).[29] A planar layer of $CH_3NH_3PbI_3$ ($MAPI_3$) was deposited from a 3:1 solution of methylammonium iodide and lead acetate as described elsewhere,[30] resulting in a uniform and continuous perovskite layer as confirmed by SEM (Figure 1a). In addition to spiro-OMeTAD, five organic small molecules were chosen with a range of IPs for use as HTMs for these devices (Supporting Information (SI) Figure 1). These molecules were chosen for their range in IP, their wide band gap to ensure selectivity (SI Figure 4), their demonstrated processing by thermal evaporation, and their previous use as contact layers in perovskite- or organic-based devices.[12,31] Measured IPs of the selected small molecules range from 5.0 to 5.5 eV,[12,21,31] meaning that the highest-occupied molecular orbital (HOMO) of these various molecules will either encourage or be a barrier to charge extraction depending upon the molecule.

All HTMs except for spiro-OMeTAD were deposited as a 15 nm thick conformal layer via thermal evaporation, removing the complexities of solution processing. To increase the conductivity of these films, 5 nm of MoO_3 was evaporated onto the HTMs, leveraging the remote-doping effect recently demonstrated by Sargent et al.[32]

Completed devices were tested to determine the effect of the HTM IP on the photovoltaic performance (Figure 2 and Table 1). The majority of HTMs employed in this study (meoTPD, spiroTTB, spiroTAD, α-NPD, and spiro-OMeTAD) showed comparable efficiency, with champion power conversion efficiencies of ~14% (SI Table 1) and minimal current–voltage hysteresis for these evaporated HTMs (SI Figure 2). While these device efficiencies are significantly lower than those of record perovskite devices employing titania scaffolds and

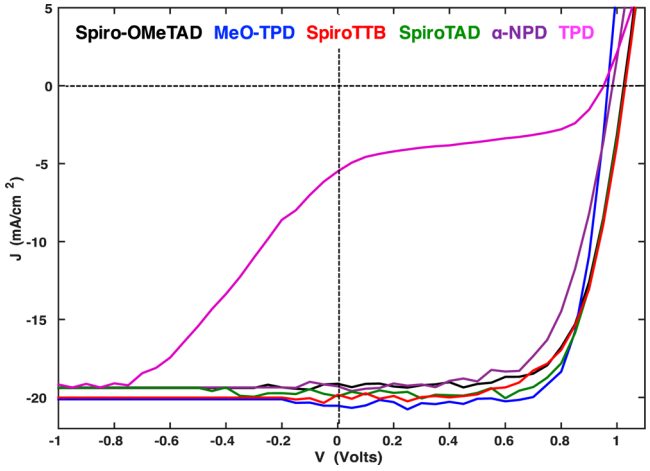

Figure 2. Current–voltage characteristics of champion perovskite devices made with alternative HTMs taken at 0.025 V/s from forward to reverse bias.

more complicated perovskite chemistries, they are comparable to the best device efficiencies for solar cells using the lead-acetate deposition method that was chosen by this study for its reproducibility.[30,33]

Of all of the devices, only those made with TPD performed significantly differently. The uniqueness of TPD can be explained by the formation of an extraction barrier at the perovskite/HTM interface, as clearly indicated by the sharp s-kink *JV* characteristic and the restoration of the photocurrent at large reverse bias.[34] This behavior is unsurprising given that the IP of TPD was the largest of the HTMs (as determined by photoemission spectroscopy in air) at approximately 5.4 eV (SI Figure 3).

For devices with IPs within the band gap of $MAPbI_3$, the variation in performance is minimal. All devices have similar photocurrents, suggesting that a substantial energetic offset between the valence band of the perovskite and HTM is unnecessary for current collection. The open-circuit voltage, which is most often predicted to increase with deeper IP, only exhibits improvement on the order of tens of mV. When replacing MeO-TPD with spiro-TTB, the HTM IP is shifted by 150 mV, but the V_{OC} is only improved by 40 mV. As the HTM

DOI: 10.1021/acsenergylett.6b00270
ACS Energy Lett. 2016, 1, 556–560

Table 1. Average Solar Cell Performance for Devices Made with HTMs with Varying IPs

HTM	IP (eV)	J_{sc} (mA/cm^2)	V_{oc} (V)	FF	PCE (%)
spiro-OMeTAD	5.15	−19.6 ± 0.3	1.02 ± 0.02	0.65 ± 0.04	13.0 ± 1.5
meoTPD	5.10	−19.8 ± 1.0	0.96 ± 0.02	0.68 ± 0.06	13.9 ± 1.7
spiroTTB	5.25	−20.7 ± 0.4	1.00 ± 0.03	0.67 ± 0.07	13.9 ± 1.7
spiroTAD	5.30	−20.3 ± 0.6	1.00 ± 0.02	0.61 ± 0.08	12.2 ± 1.8
α-NPD	5.35	−20.3 ± 0.3	0.99 ± 0.02	0.60 ± 0.08	12.2 ± 1.8
TPD	5.40	−4.4 ± 2.1	0.70 ± 0.2	0.14 ± 0.03	0.49 ± 0.3

IP is further deepened, no additional increases in V_{OC} are observed. Ultimately, the V_{OC} begins to decrease as the HOMO approaches the perovskite band edge, with α-NPD devices having comparable V_{OC} to those made with meoTPD, despite a 250 meV change in IP.

Analyzing the variation in V_{OC} with IP, it is clear that the overall response of the photovoltage of perovskite solar cells is flat; for a wide range of IPs, the V_{OC} of the perovskite is practically unaffected. Beyond the IP, the similarity in doping density for the evaporated HTMs used in this study suggests that the V_{OC} of these perovskite devices is independent of the HTM work function as well (as estimated by conductivity data in SI Table 2). According to the Fermi-level approximation for nondegenerate semiconductors, by assuming a similar density of states, we can relate a constant carrier density to a fixed energetic offset between the HTM valence band and HTM work function; therefore, the work function of our evaporated HTMs should shift in step with the IP. The constant V_{OC} reported here stands in sharp contrast to trends previously observed for dye-sensitized solar cells, where changing the redox potential of the electrolyte or shifting the alignment of the TiO_2/dye interface to more closely match the HOMO and LUMO of the dye had strong effects on V_{OC}.[35,36] The trend observed here is similar to behavior formerly seen for light-emitting electrochemical cells and photoelectrochemical cells, where the performance and photovoltages of the devices are independent of the contact work function and electrolyte redox potential, respectivelty.[37,38]

The explanation for this observed phenomenon in photoelectrochemical cells is ionic accumulation at the semiconductor surface, and it is a possible explanation for the V_{OC} trend observed here for perovskite solar cells. For these semiconductor−electrolyte junctions, there is sufficient charge at the semiconductor surface that any potential that would be dropped over the bulk of the semiconductor at the forming of a heterojunction is instead entirely dropped over a thin ionic layer near the surface. This results in a Fermi-level position within the semiconductor that is independent of the work function of the adjoining material in the heterojunction, and correspondingly, the photovoltage is mostly unaffected by variation in the contact material.[37]

Surface-charge enabling a similar Fermi-level independence in perovskite solar cells could come from surface defects or surface dipoles, but perhaps a more likely candidate is the many ionic defects predicted to occur and be mobile in these materials.[39,40] In an attempt to describe the widely observed phenomena of current−voltage hysteresis, several groups have modeled the perovskite absorber as a coupled electronic−ionic conductor and have been able to explain experimentally observed *JV* phenomena with the accumulation of ionic defects, such as iodide vacancies, in thin Debye layers at the perovskite/selective contact junctions.[39,41,42] These accumulated ionic defects could compensate for any changes in potential that accompany varying the work function of the HTM, resulting in a perovskite material that is agnostic to the HTM work function and superseding the hypothesized dependence of V_{OC} on the HTM.

An example of this phenomenon is schematically represented in Figure 3, with simplified band structures for a typical PIN-type solar cell without ionic accumulation (panel a) and a solar cell with ionic accumulation (panel b), made with a deep work function HTM and at a given applied voltage (V_{ap}). In the PIN case (Figure 3a), changing the HTM work function impacts the built-in voltage (V_{bi}) in the device as well as the carrier density throughout the perovskite, particularly at the perovskite/selective contact junction. This variation in V_{bi} should not impact recombination dynamics at V_{OC} nor should the variation in carrier density with the HTM work function affect bimolecular recombination in the perovskite, which is governed by the product of the carrier densities (electrons and holes) in the material and is therefore dependent upon the quasi-Fermi-level splitting (V_{ap}) and not where those levels reside within in the band gap of the perovskite. Monomolecular recombination processes, those governed by a single carrier density, should however be affected by HTM variation and result in significant variations in V_{OC}. In the ionic accumulation case (Figure 3b), these variations in the HTM are accommodated by a vacuum-level shift (drawn here as enabled by the accumulation of positive charge such as iodide vacancies theorized to exist in these materials[43]) at the interface, screening the electric field across the perovskite and leaving carrier densities, and therefore recombination, independent of the HTM. It is important to note that the band structure described in Figure 3b is at this time a hypothesis. Further research should look to better understand the exact nature of this vacuum-level shift (whether it is indeed mobile ionic defects or perhaps specific ionic surface states) and if it can be extended to all perovskite chemistries, but if it is indeed present then independence between the perovskite Fermi-level and HTM work function would be expected.

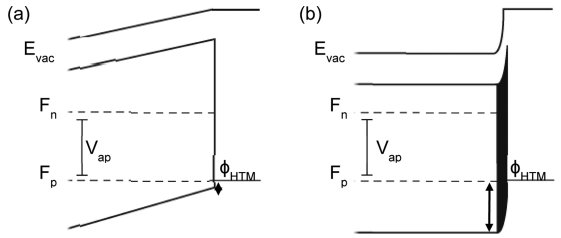

Figure 3. Schematic band structures of a HTM/perovskite heterojunction for a standard PIN-type solar cell without ion accumulation (a) compared to a schematic for the band structures of a device with the same HTM but with ionic accumulation (b).

The observation that V_{OC} is mostly independent of the HTM IP has important implications for future HTM design and

DOI: 10.1021/acsenergylett.6b00270
ACS Energy Lett. 2016, 1, 556−560

optimization. For one, it relaxes the need to develop HTMs with deeper IPs and dopants for these deep IP materials to maximize the voltage in $MAPbI_3$ devices. Our results suggest that the relatively low IP of spiro-OMeTAD is not detrimental for achieving high V_{OC}, which is, of course, reflected in its use for the highest efficiency devices; therefore, replacement materials may look to address the parasitic absorption or instability of spiro-OMeTAD instead of focusing on its IP. Second, it suggests that the pathway for improving the V_{OC} of perovskite solar cells though HTM selection is through considering the effects of the HTM on the perovskite itself. Selective contact materials can be chosen for improved perovskite morphology or for deposition procedures that maximize solvent annealing, surface coverage, or surface-passivating effects. In doing this, one can hope to improve the perovskite quality and thereby increase the possible quasi-Fermi level splitting within the perovskite material for a higher V_{OC} and power conversion efficiency.

■ ASSOCIATED CONTENT

Supporting Information

The Supporting Information is available free of charge on the ACS Publications website at DOI: 10.1021/acsenergylett.6b00270.

Experimental details; champion solar cell metrics; and HTM characterization data including molecular structure, photoemission spectroscopy data, absorption data, and conductivity data (PDF)

■ AUTHOR INFORMATION

Corresponding Author

*E-mail: mmcgehee@stanford.edu.

Notes

The authors declare no competing financial interest.

■ ACKNOWLEDGMENTS

This research was funded by the Department of Energy's Sunshot NextGen III program under Award Number DE-EE0006707. The surface characterization and microscopy were completed at the Stanford Nanocharacterization Laboratory. Additionally, the authors would like to acknowledge Nick Rolston and Kevin Bush of Stanford University for the device fabrication support and expertise.

■ REFERENCES

(1) Kojima, A.; Teshima, K.; Shirai, Y.; Miyasaka, T. Organometal Halide Perovskites as Visible-Light Sensitizers for Photovoltaic Cells. *J. Am. Chem. Soc.* **2009**, *131*, 6050−6051.

(2) Lee, M. M.; Teuscher, J.; Miyasaka, T.; Murakami, T. N.; Snaith, H. J. Efficient Hybrid Solar Cells Based on Meso-Superstructured Organometal Halide Perovskites. *Science* **2012**, *338*, 643−647.

(3) Burschka, J.; Pellet, N.; Moon, S.-J.; Humphry-Baker, R.; Gao, P.; Nazeeruddin, M. K.; Grätzel, M. Sequential Deposition as a Route to High-Performance Perovskite-Sensitized Solar Cells. *Nature* **2013**, *499*, 316−319.

(4) Liu, M.; Johnston, M. B.; Snaith, H. J. Efficient Planar Heterojunction Perovskite Solar Cells by Vapour Deposition. *Nature* **2013**, *501*, 395−398.

(5) Jeon, N. J.; Noh, J. H.; Yang, W. S.; Kim, Y. C.; Ryu, S.; Seo, J.; Seok, S. Il. Compositional Engineering of Perovskite Materials for High-Performance Solar Cells. *Nature* **2015**, *517*, 476−480.

(6) Yang, W. S.; Noh, J. H.; Jeon, N. J.; Kim, Y. C.; Ryu, S.; Seo, J.; Seok, S. I. High-Performance Photovoltaic Perovskite Layers Fabricated through Intramolecular Exchange. *Science* **2015**, *348*, 1234−1237.

(7) Bi, D.; Tress, W.; Dar, M. I.; Gao, P.; Luo, J.; Renevier, C.; Schenk, K.; Abate, A.; Giordano, F.; Correa Baena, J.-P.; et al. Efficient Luminescent Solar Cells Based on Tailored Mixed-Cation Perovskites. *Sci. Adv.* **2016**, *2*, e1501170.

(8) Zhang, W.; Saliba, M.; Moore, D. T.; Pathak, S. K.; Hörantner, M. T.; Stergiopoulos, T.; Stranks, S. D.; Eperon, G. E.; Alexander-Webber, J. A.; Abate, A.; et al. Ultrasmooth Organic−inorganic Perovskite Thin-Film Formation and Crystallization for Efficient Planar Heterojunction Solar Cells. *Nat. Commun.* **2015**, *6*, 6142.

(9) Correa Baena, J. P.; Steier, L.; Tress, W.; Saliba, M.; Neutzner, S.; Matsui, T.; Giordano, F.; Jacobsson, J.; Srimath Kandada, A. R.; Zakeeruddin, S. M.; et al. Highly Efficient Planar Perovskite Solar Cells through Band Alignment Engineering. *Energy Environ. Sci.* **2015**, *8*, 2928−2934.

(10) Ameen, S.; Rub, M. A.; Kosa, S. A.; Alamry, K. A.; Akhtar, M. S.; Shin, H.-S.; Seo, H.-K.; Asiri, A. M.; Nazeeruddin, M. K. Perovskite Solar Cells: Influence of Hole Transporting Materials on Power Conversion Efficiency. *ChemSusChem* **2016**, *9*, 10−27.

(11) Yan, W.; Ye, S.; Li, Y.; Sun, W.; Rao, H.; Liu, Z.; Bian, Z.; Huang, C. Hole-Transporting Materials in Inverted Planar Perovskite Solar Cells. *Adv. Energy Mater.* **2016**, DOI: 10.1002/aenm.201600474.

(12) Polander, L. E.; Pahner, P.; Schwarze, M.; Saalfrank, M.; Koerner, C.; Leo, K. Hole-Transport Material Variation in Fully Vacuum Deposited Perovskite Solar Cells. *APL Mater.* **2014**, *2*, 081503.

(13) Choi, H.; Park, S.; Paek, S.; Ekanayake, P.; Nazeeruddin, M. K.; Ko, J. Efficient Star-Shaped Hole Transporting Materials with Diphenylethenyl Side Arms for an Efficient Perovskite Solar Cell. *J. Mater. Chem. A* **2014**, *2*, 19136−19140.

(14) Cheng, M.; Xu, B.; Chen, C.; Yang, X.; Zhang, F.; Tan, Q.; Hua, Y.; Kloo, L.; Sun, L. Phenoxazine-Based Small Molecule Material for Efficient Perovskite Solar Cells and Bulk Heterojunction Organic Solar Cells. *Adv. Energy Mater.* **2015**, *5*, 1401720.

(15) Kim, G.-W.; Kang, G.; Kim, J.; Lee, G.-Y.; Kim, H. Il; Pyeon, L.; Lee, J.; Park, T. Dopant-Free Polymeric Hole Transport Materials for Highly Efficient and Stable Perovskite Solar Cells. *Energy Environ. Sci.* **2016**, *9*, 2326−2333.

(16) Song, Y.; Lv, S.; Liu, X.; Li, X.; Wang, S.; Wei, H.; Li, D.; Xiao, Y.; Meng, Q. Energy Level Tuning of TPB-Based Hole-Transporting Materials for Highly Efficient Perovskite Solar Cells. *Chem. Commun.* **2014**, *50*, 15239−15242.

(17) Lim, K. G.; Kim, H. B.; Jeong, J.; Kim, H.; Kim, J. Y.; Lee, T. W. Boosting the Power Conversion Efficiency of Perovskite Solar Cells Using Self-Organized Polymeric Hole Extraction Layers with High Work Function. *Adv. Mater.* **2014**, *26*, 6461−6466.

(18) Ryu, S.; Noh, J. H.; Jeon, N. J.; Chan Kim, Y.; Yang, W. S.; Seo, J.; Seok, S. Il. Voltage Output of Efficient Perovskite Solar Cells with High Open-Circuit Voltage and Fill Factor. *Energy Environ. Sci.* **2014**, *7*, 2614−2618.

(19) Kulbak, M.; Cahen, D.; Hodes, G. How Important Is the Organic Part of Lead Halide Perovskite Photovoltaic Cells? Efficient $CsPbBr_3$ Cells. *J. Phys. Chem. Lett.* **2015**, *6*, 2452−2456.

(20) Zhang, J.; Xu, B.; Johansson, M. B.; Vlachopoulos, N.; Boschloo, G.; Sun, L.; Johansson, E. M. J.; Hagfeldt, A. Strategy to Boost the Efficiency of Mixed-Ion Perovskite Solar Cells: Changing Geometry of the Hole Transporting Material. *ACS Nano* **2016**, *10*, 6816−6825.

(21) Schulz, P.; Edri, E.; Kirmayer, S.; Hodes, G.; Cahen, D.; Kahn, A. Interface Energetics in Organo-Metal Halide Perovskite-Based Photovoltaic Cells. *Energy Environ. Sci.* **2014**, *7*, 1377−1381.

(22) Harwell, J. R.; Baikie, T. K.; Baikie, I. D.; Payne, J. L.; Ni, C.; Irvine, J. T. S.; Turnbull, G. A.; Samuel, I. D. W. Probing the Energy Levels of Perovskite Solar Cells via Kelvin Probe and UV Ambient Pressure Photoemission Spectroscopy. *Phys. Chem. Chem. Phys.* **2016**, *18*, 19738−19745.

(23) Nguyen, W. H.; Bailie, C. D.; Unger, E. L.; McGehee, M. D. Enhancing the Hole-Conductivity of Spiro-OMeTAD without Oxygen

DOI: 10.1021/acsenergylett.6b00270
ACS Energy Lett. 2016, 1, 556−560

or Lithium Salts by Using Spiro(TFSI)$_2$ in Perovskite and Dye-Sensitized Solar Cells. *J. Am. Chem. Soc.* **2014**, *136*, 10996−11001.
(24) Abate, A.; Planells, M.; Hollman, D. J.; Barthi, V.; Chand, S.; Snaith, H. J.; Robertson, N. Hole-Transport Materials with Greatly-Differing Redox Potentials Give Efficient TiO2-[CH_3NH_3][PbX_3] Perovskite Solar Cells. *Phys. Chem. Chem. Phys.* **2015**, *17*, 2335−2338.
(25) Hou, Y.; Chen, W.; Baran, D.; Stubhan, T.; Luechinger, N. A.; Hartmeier, B.; Richter, M.; Min, J.; Chen, S.; Quiroz, C. O. R.; et al. Overcoming the Interface Losses in Planar Heterojunction Perovskite-Based Solar Cells. *Adv. Mater.* **2016**, *28*, 5112−5120.
(26) Zhao, D.; Sexton, M.; Park, H.-Y.; Baure, G.; Nino, J. C.; So, F. High-Efficiency Solution-Processed Planar Perovskite Solar Cells with a Polymer Hole Transport Layer. *Adv. Energy Mater.* **2015**, *5*, 1401855.
(27) Noel, N. K.; Abate, A.; Stranks, S. D.; Parrott, E. S.; Burlakov, V. M.; Goriely, A.; Snaith, H. J. Enhanced Photoluminescence and Solar Cell Performance via Lewis Base Passivation of Organic-Inorganic Lead Halide Perovskites. *ACS Nano* **2014**, *8*, 9815−9821.
(28) Kim, J. H.; Liang, P.; Williams, S. T.; Cho, N.; Chueh, C.; Glaz, M. S.; Ginger, D. S.; Jen, A. K. High-Performance and Environmentally Stable Planar Heterojunction Perovskite Solar Cells Based on a Solution-Processed Copper-Doped Nickel Oxide Hole-Transporting Layer. *Adv. Mater.* **2015**, *27*, 695−701.
(29) Shao, Y.; Xiao, Z.; Bi, C.; Yuan, Y.; Huang, J. Origin and Elimination of Photocurrent Hysteresis by Fullerene Passivation in $CH_3NH_3PbI_3$ Planar Heterojunction Solar Cells. *Nat. Commun.* **2014**, *5*, 5784.
(30) Zhang, W.; Pathak, S.; Sakai, N.; Stergiopoulos, T.; Nayak, P. K.; Noel, N. K.; Haghighirad, A. A.; Burlakov, V. M.; deQuilettes, D. W.; Sadhanala, A.; et al. Enhanced Optoelectronic Quality of Perovskite Thin Films with Hypophosphorous Acid for Planar Heterojunction Solar Cells. *Nat. Commun.* **2015**, *6*, 10030.
(31) Shinmura, Y.; Kubo, M.; Kaji, T.; Hiramoto, M. Improvement of Photovoltaic Characteristics by MoO_3 Doping of Thick Hole-Transporting Films. *Jpn. J. Appl. Phys.* **2013**, *52*, 04CR12.
(32) Xu, J.; Voznyy, O.; Comin, R.; Gong, X.; Walters, G.; Liu, M.; Kanjanaboos, P.; Lan, X.; Sargent, E. H. Crosslinked Remote-Doped Hole-Extracting Contacts Enhance Stability under Accelerated Lifetime Testing in Perovskite Solar Cells. *Adv. Mater.* **2016**, *28*, 2807−2815.
(33) Bush, K. A.; Bailie, C. D.; Chen, Y.; Bowring, A. R.; Wang, W.; Ma, W.; Leijtens, T.; Moghadam, F.; McGehee, M. D. Thermal and Environmental Stability of Semi-Transparent Perovskite Solar Cells for Tandems Enabled by a Solution-Processed Nanoparticle Buffer Layer and Sputtered ITO Electrode. *Adv. Mater.* **2016**, *28*, 3937−3943.
(34) Tress, W.; Leo, K.; Riede, M. Influence of Hole-Transport Layers and Donor Materials on Open-Circuit Voltage and Shape of I-V Curves of Organic Solar Cells. *Adv. Funct. Mater.* **2011**, *21*, 2140−2149.
(35) Kang, S. H.; Kim, J.-Y.; Kim, Y.; Kim, H. S.; Sung, Y.-E. Surface Modification of Stretched TiO_2 Nanotubes for Solid-State Dye-Sensitized Solar Cells. *J. Phys. Chem. C* **2007**, *111*, 9614−9623.
(36) Feldt, S. M.; Gibson, E. A.; Gabrielsson, E.; Sun, L.; Boschloo, G.; Hagfeldt, A. Design of Organic Dyes and Cobalt Polypyridine Redox Mediators for High-Efficiency Dye-Sensitized Solar Cells. *J. Am. Chem. Soc.* **2010**, *132*, 16714−16724.
(37) Bard, A. J.; Bocarsly, A. B.; Fan, F. R. F.; Walton, E. G.; Wrighton, M. S. The Concept of Fermi Level Pinning at Semiconductor/liquid Junctions. Consequences for Energy Conversion Efficiency and Selection of Useful Solution Redox Couples in Solar Devices. *J. Am. Chem. Soc.* **1980**, *102*, 3671−3677.
(38) Yang, Y.; Pei, Q. Voltage Controlled Two Color Ligh-Emitting Electrochemical Cells. *Appl. Phys. Lett.* **1996**, *68*, 2708−2710.
(39) Eames, C.; Frost, J. M.; Barnes, P. R. F.; O'Regan, B. C.; Walsh, A.; Islam, M. S. Ionic Transport in Hybrid Lead Iodide Perovskite Solar Cells. *Nat. Commun.* **2015**, *6*, 7497.
(40) Walsh, A.; Scanlon, D. O.; Chen, S.; Gong, X. G.; Wei, S.-H. Self-Regulation Mechanism for Charged Point Defects in Hybrid Halide Perovskites. *Angew. Chem.* **2015**, *127*, 1811−1814.
(41) Richardson, G.; O'Kane, S. E. J.; Niemann, R. G.; Peltola, T. A.; Foster, J. M.; Cameron, P. J.; Walker, A. B. Can Slow-Moving Ions Explain Hysteresis in the Current−voltage Curves of Perovskite Solar Cells? *Energy Environ. Sci.* **2016**, *9*, 1476−1485.
(42) van Reenen, S.; Kemerink, M.; Snaith, H. J. Modeling Anomalous Hysteresis in Perovskite Solar Cells. *J. Phys. Chem. Lett.* **2015**, *6*, 3808−3814.
(43) Yin, W.-J.; Shi, T.; Yan, Y. Unusual Defect Physics in $CH_3NH_3PbI_3$ Perovskite Solar Cell Absorber. *Appl. Phys. Lett.* **2014**, *104*, 063903.

DOI: 10.1021/acsenergylett.6b00270
ACS Energy Lett. 2016, 1, 556−560